Aβ oligomers induce sex-selective pathophysiological mGluR5 signaling in Alzheimer mice

Khaled S. Abd-Elrahman[1,2,6,#], Awatif Albaker[1,2,7,#], Jessica M. de Souza[1,2,8], Fabiola M. Ribeiro[8], Michael G. Schlossmacher[1,2,3,5], Mario Tiberi[1,2,4,5], Alison Hamilton[1,2.$] and Stephen S. G. Ferguson[1,2,$,*]

[1]University of Ottawa Brain and Mind Institute, [2]Departments of Cellular and Molecular Medicine, [3] Medicine, [4]Psychiatry, and the [5]Ottawa Hospital Research Institute, University of Ottawa, Ottawa, Ontario, K1H 8M5, Canada.

[6]Department of Pharmacology and Toxicology, Faculty of Pharmacy, Alexandria University, Alexandria, 21521, Egypt.

[7]Department of Pharmacology and Toxicology, College of Pharmacy, King Saud University, Riyadh, 12371, Saudi Arabia

[8]Department of Biochemistry and Immunology, ICB, Universidade Federalde Minas Gerais, Belo Horizonte, Brazil.

[#]These authors contributed equally

[$] Co-senior authors

*Corresponding author

Dr. Stephen S. G. Ferguson

Department of Cellular and Molecular Medicine, University of Ottawa,

451 Smyth Dr. Ottawa, Ontario, Canada, K1H 8M5.

Tel: (613) 562 5800 Ext 8889.

sferguso@uottawa.ca

ABSTRACT

Sex is a key modifier of the prevalence and progression of Alzheimer's disease (AD) and mGluR5 is linked to AD progression. We show that mGluR5 inhibition reverses cognitive decline and β-amyloid (Aβ) oligomer pathology that was paralleled by reactivation of GSK3β/ZBTB16-regulated autophagy in male, but not female, APPswe/PS1ΔE9 mice. Aβ oligomers via mGluR5 inhibits ZBTB16-regulated autophagy in male neuronal cultures only. Aβ oligomers binds with high-affinity to endogenous mGluR5 from male, but not female, mouse and human brain. Aβ oligomer binding to mGluR5 is dependent on cellular prion protein (PrP^c) as mGluR5 co-immunoprecipitates with PrP^c from male, but not female, mouse brain. Thus, the mGluR5/Aβ oligomer/PrP^c ternary complex contributing to aberrant Aβ oligomer signaling in males, but does not contribute to disease pathology in females. This study highlights the complexity of mGluR5 pharmacology and Aβ oligomer-activated pathological signaling and emphasizes the need for clinical trials redesign and analysis of sex-tailored treatment for AD.

KEY WORDS: Alzheimer's disease, autophagy, mGluR5, sex, Beta Amyloid, PrPc

INTRODUCTION

Alzheimer's disease (AD) is a progressive neurodegenerative disease characterized by age-related memory loss and cognitive decline and despite the alarming prevalence, no available treatments exist to either modify or reverse its progression [1–3]. β-Amyloid (Aβ) oligomers and hyper-phosphorylated tau protein represent pathological hallmarks of AD and accumulate with disease progression to disrupt neuronal signaling and trigger neurodegeneration [4–6]. Sex is an important modulator of AD prevalence and both clinical and preclinical evidence indicate that the incidence in females is higher than age- and risk factor-matched males [7–10]. This higher incidence of cognitive impairment is commonly attributed to reduced estrogen and/or estrogen receptors levels following menopause [11–13]. However, this assumption was weakened by the first large-scale clinical study demonstrating increased risk of dementia and poor cognitive outcomes following hormone-replacement therapy (Women's Health Initiative Memory Study, WHIMS) [14,15]. This finding along with the dramatic failure rate in AD clinical trials [10,16] warrant investigating the differential modulation of the pathophysiological mechanism(s) underlying AD in both sexes.

Glutamate, the main excitatory brain neurotransmitter, plays a key role in learning and memory and the $G_{\alpha q}$-coupled metabotropic glutamate receptors 5 (mGluR5) is of particular interest in AD pathology [5,17]. mGluR5 functions as an extracellular scaffold for Aβ and cellular prion protein (PrP^c) and the complex between PrP^c and mGluR5 is essential for Aβ binding [18–20]. Aβ also promotes mGluR5 clustering, increases intracellular Ca^{2+} release and inhibits autophagy [18,20,21]. More so, the pharmacological and genetic silencing of mGluR5 reverses cognitive deficits and reduces Aβ pathology in male AD rodent models [21–25]. While these studies emphasized the key role of mGluR5 in AD pathophysiology in male models of AD, it is not yet clear whether alterations in mGluR5 signaling are conserved between male and female AD models.

Since both clinical and experimental evidence indicated a divergent AD pathology in males and female, we tested here whether the mGluR5 orally bioavailable negative allosteric modulator

(NAM), 2-chloro-4-((2,5-dimethyl-1-(4-(trifluoromethoxy)phenyl)-1H-imidazol-4-yl)ethynyl) pyridine (CTEP) [26], improves cognition and reduces soluble Aβ in both male and female APPswe/PS1ΔE9 (APP) mice [27]. We found that, while CTEP treatment improved cognitive function, reduced pathology and enhanced autophagy signaling in male APP mice, the drug was completely ineffective for treating female APP mice. To control for hormonal differences, we employed wild-type male and female E18 embryonic neuronal cultures. The treatment of male cultures with Aβ oligomers resulted in an increase in pS9-GSK3β phosphorylation resulting in antagonism of a GSK3β/ZBTB16-mediated autophagic signaling. In contrast, the treatment of female cultures with Aβ oligomers did not alter pS9-GSK3β phosphorylation status and had no effect on autophagy. More so, Aβ oligomers displaced [^{3}H]-MPEP binding to mGluR5 in both male mouse and human cortex with high affinity, but exhibited no affinity for mGluR5 in either female mice or female human brain tissue. The binding of Aβ oligomers to mGluR5 was PrP^c-dependent as mGluR5 co-immunoprecipitated with PrP^c from male, but not female, mouse hippocampus. These studies revealed that mGluR5 exhibits unexpected and distinct pharmacological profiles with respect to Aβ oligomer/PrP^c interactions in male and female brain.

RESULTS

mGluR5 blockade improved cognitive deficits in male, but not female, APP mice

We assessed whether chronic mGluR5 inhibition would improve memory impairments in age-matched male and female APP mice. Six-month-old male and female wild-type (Wt) and APP mice were treated for 12 weeks with CTEP (2 mg/Kg) and then tested for impairments in working and spatial memory in the novel object recognition test and the Morris water maze (MWM) and Morris water maze with reversal (RMWM). In the novel object recognition test, vehicle-treated Wt male and female mice discriminated between novel and familiar objects, whereas vehicle-treated male and female APP mice failed to discriminate between objects (Fig. 1a and 2b). Following CTEP treatment, male APP mice regained the capacity to discriminate between objects, whereas female APP mice remained cognitively impaired (Fig. 1a and 1b). When mice were tested in open field, it was evident that the discrepancies in cognitive function between CTEP-treated male and female mice cannot be attributed to difference in locomotor behavior (Fig. 1c and 1d). In MWM and RMWM, vehicle-treated male and female APP mice exhibited significantly longer escape latencies, greater path lengths and less time spent in target quadrant than did similarly treated same sex Wt mice (Fig.2a-h). CTEP treatment improved male APP mice performance in both the MWM and RMWM as measured by shorter escape latency, path length and longer time spent in target quadrant with values indistinguishable from Wt mice (Fig. 1a-h). In contrast, CTEP treatment did not improve either escape latency, path length, swim speed or time spent in target quadrant of female APP mice in either the MWM or RMWM, when compared to vehicle-treated female APP mice (Fig. 1a-h). CTEP treatment also impaired female wild-type mouse performance in the RMWM compared to vehicle-treated Wt mice (Fig. 1e-h). Therefore, male and female APP mice presented with a similarly impaired cognitive phenotype, but chronic CTEP treatment improved cognitive performance in male, but not female, mice.

mGluR5 inhibition reduced AD-related pathology in male, but not female, APP mice

We tested whether the sex-specific CTEP-dependent improvement of cognitive function in APP mice was paralleled by changes in Aβ pathology. The deposition of Aβ plaque density was significantly reduced in male, but not female, APP mouse cortical and hippocampal slices following CTEP treatment (Fig. 3a and 3b). Soluble Aβ levels detected in brain lysates from both male and female APP mice were comparably increased versus sex-matched Wt mice and CTEP treatment reduced soluble Aβ in male, but not female, APP mice (Fig. 3c).

We have previously demonstrated that clearance of proteotoxic aggregates can be enhanced by inhibiting pathological mGluR5 signaling and activating a novel Glycogen Synthase Kinase 3β (GSK3β)/ Zinc Finger and BTB Domain Containing 16 (ZBTB16)/ Autophagy Related 14 (ATG14) autophagy pathway in male mice [21,28,29]. Here, we found that the GSK3β/ZBTB16/ ATG14 autophagy pathway was inhibited in vehicle treated male, but not female, APP mice (Fig. 3d-g). The cell signaling hallmarks of GSK3β/ZBTB16/ATG14 pathway inhibition are increased pS9-GSK3β level, increased ZBTB16 expression, reduced ATG14 expression and the accumulation of p62 protein (Fig. 3d-g) [21,28,29]. CTEP treatment attenuated pS9-GSK3β phosphorylation, thereby activating autophagy in male APP mice whereas, it had absolutely no effect in female APP mice (Fig. 3d-g). Overall, we showed that while defects in autophagic clearance of Aβ contribute to AD-like neuropathology in both sexes of APP mice, the contribution of pathological mGluR5 signaling to Aβ pathology was exclusive to male mice.

Sex-specific Aβ-activated mGluR5 signaling in primary embryonic neuronal cultures

Since Aβ oligomers can induce clustering and pathological activation of mGluR5 [18,20], we tested whether Aβ oligomers via mGluR5 can inactivate GSK3β/ZBTB16/ATG14 autophagy pathway in a sex-specific manner independent of the influence of sex hormones. Therefore, we examined Aβ-mediated signaling in primary wild-type male and female E18 mouse cortical

neuronal cultures. The purpose of using embryonic cultures was to avoid potentially confounding effects of sex hormones on mGluR5 signaling. Sex of the cultures was determined by PCR amplification to detect X chromosome-linked *Rbm31* gene relative to its divergent Y chromosome gametolog [30] (Fig. 4a). Treatment of male, but not female, cultures with Aβ oligomers (100 nM) induced pS9-GSK3β phosphorylation, increased ZBTB16 expression and inhibited autophagy as measured by elevated p62 expression in a manner that was inhibited by CTEP (10 μM) (Fig. 3B). These results clearly demonstrated that Aβ oligomers inactivated autophagic signaling in male, but not female, neurons in a sex hormone-independent, but mGluR5-dependent manner.

Sex-specific Aβ and PrP^c interactions with mGluR5

We then explored the underlying sex-dependent mechanism for Aβ oligomer-activated mGluR5 signaling by performing radioligand binding experiments. We assessed Aβ oligomer-mediated displacement of radiolabeled mGluR5 antagonist (MPEP) binding to endogenously expressed mGluR5 in plasma membrane preparations from mouse and human brain. Interestingly, Aβ oligomers binding assays revealed the distinct sex-dependent pharmacological profile of mGluR5. Specifically, Aβ effectively displaced [^{3}H]-MPEP binding to male, but not female mouse cortical membranes (Fig. 5a and 5b). The displacement of [^{3}H]-MPEP binding by non-radioactive MPEP was identical between both sexes (Fig. 5a and 5b). We also performed [^{3}H]-MPEP binding displacement assays in cortical membranes prepared from both male and female human cortical brain samples obtained at autopsy. Identical to what was observed for mouse cortical membranes, MPEP displaced [^{3}H]-MPEP binding to both male and female human cortical membranes, but Aβ oligomers only displaced [^{3}H]-MPEP binding to male membranes (Fig. 5c).

Aβ oligomers binds with high affinity to PrP^c and the Aβ oligomer/PrP^C complex can then drive the pathological signaling of mGluR5 [18]. We first confirmed that the Aβ oligomers that we employed bind to mGluR5 in a PrP^c-dependent manner. We found that Aβ oligomers did not displace [^{3}H]-MPEP binding in PrP^c null (CF10) cells transfected with mGluR5, but co-transfection

of CF10 cells with PrP^c and mGluR5 restored Aβ oligomer binding to mGluR5 (Fig. 5d). We then tested whether PrP^c binding to mGluR5 was different between sexes and found that mGluR5 co-immunoprecipitated with PrP^c from male, but not female, mouse hippocampal tissue (Fig. 5e). Binding specificity of PrP^c antibody to mGluR5 was validated by the lack of receptor immunoprecipitation in $mGluR5^{-/-}$ mice. Taken together, our findings indicated that the pathological mGluR5/ Aβ oligomer/PrP^c ternary complex neither forms nor contributes to AD pathology in female brain (summarized in Fig. 6).

DISCUSSION

One major challenge in AD therapy is the identification of a pharmaceutical target that both manages disease symptomology and modifies disease progression. Genetic and pharmacological silencing of mGluR5 has identified a contributory role for mGluR5 in Aβ-related cognitive decline and pathology in male AD mice [22,23]. However, gender-specific responses to therapies have been reported in many neurological diseases including AD which have the potential to further complicate the process of drug discovery [7,8,10]. We show here, that treatment of APP mice with a mGluR5 NAM improved cognitive deficits and reduced Aβ-related pathology in males, but was ineffective in females despite a similar disease phenotype. This can be attributed to the inability of mGluR5 to scaffold both Aβ oligomers and PrP^c and elicit pathological mGluR5-dependent signaling in female mouse brain tissue. This failure to form a mGluR5-scaffolded complex and Aβ oligomers to bind mGluR5 is conserved in both mouse and human female cortical tissue and represents an unexpected, but novel sex-specific regulation of mGluR5 pharmacology and signaling that appears to be evolutionarily conserved. This study has major implications as it shows how GPCRs, the most common class of receptors targeted by prescription drugs [31], can exhibits district gender-specific pharmacological profiles that must be considered in the process of drug development.

We and others have previously reported that both mGluR5 negative and silent allosteric modulators improve cognitive function in male APP mice, but only NAMs reduce Aβ oligomer-related pathology [23,32]. This combined data suggests the possibility of repurposing mGluR5 selective modulators for treatment of male AD patients. This is of particular interest since the mGluR5 NAM basimglurant has been shown to be well-tolerated by patients in clinical studies for Fragile X mental retardation and major depressive disorder [33,34]. However, a critical drawback for repurposing mGluR5 selective drugs to treat AD in the general population is that mGluR5 fails to interact with Aβ oligomers in female tissue and therefore, mGluR5 contribution to cognitive decline

and AD pathology in females is not significant. Nevertheless, important opportunities still exist for the treatment of AD in men by mGluR5-selective drugs.

Aβ oligomers are a normal proteolytic byproduct of amyloid precursor protein metabolism and are normally found at low levels in the brain. Alterations in the production and/or clearance of Aβ oligomers can shift the homeostasis towards increased cellular Aβ oligomer levels and accelerate neurodegeneration [4,35]. Therefore, enormous effort has been directed toward identifying novel pathways that can regulate Aβ oligomer accumulation. Within this context, autophagy represents an essential protein degradation pathway and defects in autophagy were reported in the early stages of AD in both animal models and patients [36–40]. We find that mGluR5 triggers pathological inhibition of autophagy via a ZBTB16-Cullin3-Roc1 E3-ubiquitin ligase pathway [29] in male, but not female, APP mice. The antagonism of mGluR5 was associated with improved cognitive function and reduced Aβ pathology in male APP mice, but unfortunately this improvement was not observed in female mice.

The ability of PrP^c and Aβ oligomers to form a scaffolding complex with male mGluR5 can promote receptor clustering at the synapses [18,20] and prevent the constitutive receptor endocytosis [41] leading to the pathological activation of mGluR5. Aβ-activated mGluR5 inhibits autophagy and can trigger a feedforward mechanism leading to further accumulation of Aβ oligomers and exacerbation of glutamatergic excitotoxicity. mGluR5 NAM via its binding to the allosteric site of mGluR5, may disrupt the interaction between Aβ oligomers and the receptor and consequently interrupt receptor-activated neurodegeneration. In fact, we have previously reported that mGluR5 NAM treatment normalizes the increased cell surface expression of mGluR5 in male APP mice [21]. The lack of PrP^c/Aβ oligomer binding to female mGluR5 means that this feedforward mechanism cannot be initiated and therefore nullify the contribution of pathological mGluR5 to AD pathophysiology in female mice,

Our *a piori* expectation predicted that mGluR5 antagonism would be equally effective in both males and females, as there have been no reported differences in either gene editing or genomic regulation of male versus female mGluR5 expression, subcellular localization and/or function. Thus, one of the major challenges of AD research remains understanding the underlying pharmacological and physiological differences in the manifestation of AD pathology in males versus females, in both animal AD mice and human patients. The sex-dependent regulation of the formation of the mGluR5/Aβ oligomer/PrP^c complex is clearly one of the underlying mechanisms for why mGluR5 antagonism is not effective in the treatment of cognitive impairment and Aβ pathology in female mice. However, this leaves open the question as to what is the underlying biological reason for why mGluR5 exhibits differential pharmacological properties in neurons of both sexes. Metabotropic glutamate receptors are allosterically regulated receptors and thus their pharmacological function may be regulated by differential interactions with either intra- or extracellular regulatory proteins in male and female [17,42]. Although estrogen receptors represent the obvious regulator of sex-specific mGluR5 signaling and pharmacology [11,12], we have been unable to provide evidence to support this hypothesis in our studies. Specifically, Aβ activated pS9-GSK3β phosphorylation to inhibit autophagy *in vitro* in male, but not female, neurons in absence of the influence of sex hormones.

The pharmacology underlying disease etiology and progression regulated by cellular processes that are independent of mGluR5 in females remains to be determined. The important underlying message from the current study is that mGluR5 is not a contributor to disease progression and pathology in female mice, thereby severely limiting the use of mGluR5 antagonists in women. However, it is important to acknowledge that mGluR5 is not the only cell surface target for Aβ oligomers and a multicity of different targets can contribute to sex-dependent and -independent changes in synaptic signaling, synaptic pruning, autophagy and neuronal cell death in female AD [43]. Given the role of mGluR5 in cognitive function [5] and the poor cognitive

performance of mGluR5 NAM-treated control female mice, it will be essential to exploit other aspects of altered mGluR5 signaling in females.

In summary, mGluR5 antagonism reduces cognitive impairment and Aβ pathology in male, but not female, AD mice. We also report that sex-specific differences in mGluR5 pharmacology observed in mouse cortical tissue are mirrored in human cortex. Our data clearly demonstrates that mGluR5 does not represent an effective pharmacological target for the treatment of AD in women, but that it still remains a potentially effective target for the treatment of the early stages of AD in men. This highlights the need for the sexual stratification of neurodegenerative drug trial result to aid in the development of sex-specific therapeutic strategies.

ACKNOWLEDGMENTS

S.S.G.F is a Tier I Canada Research Chair in Brain and Mind. K.S.A is a Lecturer at the Department of Pharmacology and Toxicology, Faculty of Pharmacy, Alexandria University. Thanks to Shaunessy Hutchinson for breeding the mouse colony, the Behavior and Physiology core at the University of Ottawa, Bassam Albraidy for technical assistance, Dr. Suzette Priola (NIH) for providing CF10 cells, Dr. Andrew West (Duke Univ.), Dr. Jennifer Chan (Univ. Calgary) and Dr. John Woulfe (The Ottawa Hospital) for their assistance in procuring human tissues. This study was supported by Canadian Institutes for Health Research (CIHR) grants (PJT-148656 and PJT-165967) and Funding from Krembil Foundation to S.S.G.F, and a Clinician Postdoctoral Fellowship from the Alberta Innovates Health Solutions (AIHS) and CIHR to K.S.A.

AUTHOR CONTRIBUTIONS

Conceptualization, K.S.A., A.H. and S.S.G.F; Methodology, Formal analysis and investigation, K.S.A., A.A., J.M.D. and A.H.; Resources, F.M.R., M.G.S., M.T., S.S.G.F.; Writing-Original draft, K.S.A.; Writing-Review & Editing, K.S.A., S.S.G.F.; Supervision and Funding acquisition, S.S.G.F.

DATA AVAILABILITY: The published article includes all datasets generated or analyzed during this study.

DECLARATION OF INTERETS: Authors declare no interests.

.

FIGURE LEGENDS

Fig. 1: CTEP improves recognition scores in male, but not female, APP mice.

Recognition index, for exploring one novel object versus familiar object in the second day of novel object recognition test following 12 week treatment with vehicle or CTEP (2mg/kg) of 6 month old **(a)** male **(b)** female wild-type (Wt) and APP mice. **(c)** Velocity **(d)** and distance travelled following 12-week treatment with vehicle or CTEP of 6 month old male and female Wt and APP mice. Data represents mean ± SEM (n=8-10 for each group). * P<0.05 versus familiar object assessed by two-way ANOVA and Fisher's LSD comparisons. Mice were excluded from analysis due to spontaneous death

Fig. 2: CTEP treatment improves performance of male, but not female, APP mice in MWM and RMWM.

Escape latency, path length, swim speed and time spent in the target quadrant for MWM **(a-d)** and RMWM **(e-h)** in 6 month old male and female wild-type (Wt) and APP mice following 12 week treatment with either vehicle or CTEP (2 mg/kg). Data represents mean ± SEM (n=8-10 for each group). *P<0.05 vs vehicle-treated Wt, $^{\#}$P<0.05 versus CTEP-treated Wt assessed by two-way ANOVA and Fisher's LSD comparisons. Mice excluded from analysis were due to spontaneous death.

Fig. 3: CTEP reduces Aβ pathology and activate autophagy in male, but not female, APP mice.

(a) Representative images of Aβ staining and **(b)** plaque density in cortical and hippocampal brain slices quantified of 5 different 900 μm^2 regions from 6 brain slices per mouse (scale bar = 1 mm), *P<0.05 vs vehicle-treated same sex APP assessed by Student's t-test. **(b)** Aβ oligomer concentrations (pg/mg) and representative immunoblots and quantification of **(d)** pS9-GSK3β, **(e)** ZBTB16, **(f)** ATG14 and **(g)** p62 with the corresponding loading controls or total protein and

expressed as a fraction of the vehicle-treated male wild-type (Wt) from 6 month old male and female Wt and APP mice treated with vehicle or CTEP (2 mg/kg) for 12 weeks. Data represents mean ± SEM (n=5 for each group). *P<0.05 vs vehicle-treated male Wt values assessed by **(b, c, e and g)** two-way ANOVA and Fisher's LSD comparisons or Kruskal-Wallis test **(d)**.

Fig. 4: Sex-specific Aβ oligomer-mediated activation of mGluR5 signaling in neuronal cultures

(a) Representative gel for the *Rbm31* gene PCR amplicon in male and female E18 wild-type (Wt) mouse embryos. **(b)** Representative immunoblots and quantification of pS9-GSK3β, ZBTB16 and p62 normalized to loading controls or total protein and expressed as a fraction of the untreated male cultures in primary cultured cortical neurons from male and female Wt E18 embryos stimulated with Aβ oligomers (100 nM) in the absence (DMSO) or presence of CTEP (10 µM). Data represents mean ± SEM (n=4 for each group). *P<0.05 versus untreated male cultures assessed by two-way ANOVA and Fisher's LSD comparisons.

Fig 5: Sex-specific Aβ oligomer and PrP^c interactions with mGluR5

[^{3}H]-MPEP displacement curves and calculated dissociation constant (K_i) for MPEP and Aβ in membrane preparations from **(a)** male wild type (Wt) mouse cortex, **(b)** female Wt mouse cortex, **(c)** male and female human cortex and **(d)** CF10 cells transfected with FLAG-mGluR5 ± PrP^c. Each binding curve represents the mean ± SEM of 3-4 independent duplicate experiments. **(e)** Representative immunoblot (IB) of mGluR5 co-immunoprecipitated with PrP^c (IP) from male and female Wt hippocampus with corresponding lysates. Hippocampal tissue from male and female $mGluR^{-/-}$ or Wt mice in the absence of mGluR5 antibody served as a negative control (n=6).

Fig 6: Schematic representation depicting Aβ oligomer induced sex-selective pathophysiological mGluR5 signaling

PrP^c forms a scaffolding complex with male mGluR5 and Aβ oligomers and elicit the inhibition of ZBTB16-mediated autophagy. The reduction in autophagic clearance of Aβ oligomers elicits pathological signaling and results in cognitive deficits. In female brain, mGluR5/Aβ oligomer/PrP^c complex is not formed and therefore pathological signaling and cognitive deficits are likely mediated by mechanism(s) other than mGluR5.

MATERIALS AND METHODS

Reagents: CTEP (1972) was purchased from Axon Medchem. β-Amyloid [1 42] PTD Human protein (03111), Amyloid beta (Aggregated) Human ELISA Kit (KHB3491), Sulfo-NHS-SS-Biotin (21331), NeutrAvidin Resins (29200), goat anti-Rabbit (G-21234) and anti-mouse (G21040) IgG (H+L) Cross-Adsorbed HRP Secondary Antibody, rabbit anti-β-Amyloid (71-5800) and rabbit anti-β-Actin (PA1-183) were from Thermo Fisher Scientific. Rabbit anti- pS9-GSK3β (9323) and mouse anti-GSK3β (9832) antibodies were from Cell Signaling Technology. Rabbit anti-ATG14L (PD026) was from MBL International. Immunoprecipitation kit (206996), mouse anti-P62 (56416), rabbit anti-vinculin (129002) and rabbit anti-ZBTB16 (39354) were from Abcam. Rabbit anti-mGluR5 (AB5675) was from Millipore. Mouse Anti-Prion Protein (PrP^c) Clone SAF-32 (189720-1) was from Cayman Chemical. [^{3}H] MPEP (VT237) was from Vitrax, MPEP (1212) was from Tocris, Effectene Transfection reagent (301425) was from Qiagen and VECTASTAIN Elite ABC HRP Kit (Rabbit IgG, PK-6101) was from Vector Laboratories. Reagents used for western blotting were purchased from Bio-Rad and all other biochemical reagents were from Sigma-Aldrich**.**

Animals: Mice were obtained from The Jackson laboratories and bred to establish littermate controlled female and male wild-type (C57BL/6J, stock# 000664), APPswe/PS1ΔE9 (B6C3-Tg (APPswe/PSEN1ΔE9)85Dbo/J, stock# 34829) and $mGluR5^{-/-}$ (B6;129-Grm5tm1Rod/J, stock# 003121) that were group-housed in cages of 2 or more animals, received food and water *ad libitum* and maintained on a 12-hour light/12hour dark cycle at 24°C. Groups of 24 male and female Wt and APPswe/PS1ΔE9 mice were aged to 6 months of age and 12 mice from each group were randomized and blindly-treated every 48h based on weekly weights with either vehicle (DMSO in chocolate pudding) or CTEP (2 mg/kg, dissolved in 10% DMSO then mixed with chocolate pudding, final DMSO concentration was 0.1%) for 12 weeks [23,28]. Cognitive function of all animals was assessed prior to and following 12 weeks of drug treatment. At the end of the 12-week treatment, mice were sacrificed by exsanguination and brains were collected and randomized for

biochemical determinations and immunostaining. Mice used for radioligand binding and coimmunoprecipitation experiments were 3 month old Wt. All animal experimental protocols were approved by the University of Ottawa Institutional Animal Care Committee and were in accordance with the Canadian Council of Animal Care guidelines.

Human specimens: All tissues were obtained collected after consent was provided from patients or the next kin in accordance with institutional review board-approved guidelines. Frozen samples of cortices from subjects under 50 years of age were acquired through the University of Alabama and the Autism Tissue Program. Additional, frozen specimens from adults above age 60 years were obtained from the Neuropathology Service at Brigham and Women's Hospital and the Department of Pathology and Laboratory Medicine at The Ottawa Hospital. Patients' gender, age and diagnosis were as follow: male, 34-year-old, vasculitis/encephalitis; male, 70-year-old, dementia with lewy bodies; male, 65-year-old, dementia with lewy bodies; male, 75-year-old, healthy; female, 44-year-old, carcinoma; female, 55-year-old, healthy; female, 65-year-old, healthy; female, 73-year-old, healthy.

Cell lines: CF10 cells were maintained in Opti-MEM supplemented with FBS (10% v/v), respectively at 37 °C in 5% CO_2 humidified incubator. CF10 cells were transfected with FLAG-mGluR5 ± PrP^c using Effectene transfection reagents following the manufacture's protocol.

Primary neuronal culture: Cultures were prepared from the cortical region of E18 male and female Wt embryo brains. Briefly, cortical tissue of each mouse embryo was trypsin-digested followed by cell dissociation using a fire-polished Pasteur pipette. Cells were plated on Poly-L-Ornithine-coated dishes in neurobasal medium supplemented with N2 and B27 supplements, 2.0 mM GlutaMAX, 50 µg/ml penicillin, and 50 µg/ml streptomycin. Cells were maintained for 12 to 15 days at 37 °C in 5% CO_2 humidified incubator before experimentation.

Experimental Methods

Novel object recognition

Mice were habituated in the testing room for 30 mins and testing was blindly performed during the animal's light cycle. Mice were placed in the empty box measuring 45 × 45 × 45 cm for 5 min and 5 min later, 2 identical objects were placed in the box 5 cm from the edge and 5 cm apart. Mice were returned to the box for 5 min, and allowed to explore, as described previously [28]. Time spent exploring each object was recorded using a camera fed to a computer in a separate room and analyzed using Noldus Ethovision 10 software. Mice were considered to be exploring an object if their snout was within 1 cm of the object. Each experiment was repeated 24 hours after first exposure with one object replaced with a novel object. Data was interpreted using recognition index which was as follows: time spent exploring the familiar object or the novel object over the total time spent exploring both objects multiplied by 100, and was used to measure recognition memory (TA or TB/ (TA + TB))*100, where T represents time, A represents familiar object and B, novel object.

Open field

Mice were habituated in the testing room for 30 mins and testing was blindly performed during the animal's light cycle. Mice were placed in in the corner of an opaque, illuminated (250–300 Lux), white box measuring 45 × 45 × 45 cm and allowed to explore for 10 min, as described previously [28]. Overhead camera fed to a computer in a separate room monitored the activity and data were analyzed using Noldus Ethovision 10 software. The distance travelled and velocity of each mouse in the open box were determined.

Morris water maze (MWM) and reversal Morris water maze (RMWM)

Animals were habituated in the testing room for 30 min and testing was blindly performed during the animal's light cycle. The Morris water maze test was performed in a white opaque plastic pool (120 cm in diameter), filled with water and maintained at 25 °C to prevent hypothermia, as described previously [23]. A clear escape platform (10 cm diameter) was placed 25 cm from the perimeter, hidden one cm beneath the surface of the water. Visual cues were placed on the walls in the room of the maze as spatial references. Mice were trained for 4 days (four trials per day and 15 mins between trails) to find the submerged platform at a fixed position from a random start point of the 4 equally spaced points around the pool. Each trial lasted either 60 seconds or until the mouse found the platform and mice remained on the platform for 15 seconds before being removed to their home cage. If the mice failed to find the platform within 60 seconds, they were guided to the platform by the experimenter. Escape latency and swim speed were measured using Ethovision 10 automated video tracking software from Noldus. On day 5, the probe trial (a single trial of 60 seconds) was performed by removing the platform and allowing the mice to swim freely in the pool and recording the time spent in the target quadrant. RMWM task was initiated 24 hours after completion of MWM using the same paradigm as MWM, with 4 days acquisition and probe trial. In the RMWM task, the platform was relocated to a new position.

Sandwich ELISA for Aβ oligomer levels

ELISA was performed as described previously [23,25]. Briefly, brains were dissected and one hemisphere was used to analyze oligomeric Aβ levels. Brain homogenates were divided and centrifuged at 4°C at 100,000 ×g for 1 hour. The supernatant was then diluted 1:10 with kit-provided buffer before carrying out the ELISA, which was performed in triplicate and measured as detailed in the manufacturer's protocol. Protein concentrations were quantified using the Bradford protein assay (Bio-Rad). The final Aβ concentrations were determined following normalization to total protein levels.

β-Amyloid immunohistochemistry

Immunostaining was performed as described previously [23,25]. Briefly, brains were coronally sectioned through the cortex and hippocampus and staining was performed on 40 µm free-floating sections using a peroxidase-based immunostaining protocol (VECTASTAIN Elite ABC HRP Kit). Sections were incubated overnight in primary antibody for Aβ (1:200) at 4 °C, washed, incubated in biotinylated antibody (biotinylated horse anti-rabbit, 1:400) for 90 mins at 4 °C, then incubated in an avidin biotin enzyme reagent for 90 min at 4°C and visualized using a chromogen. Sections were mounted on slides and visualized with a Zeiss AxioObserver epifluorescent microscope with a Zeiss 20× lens, using representative 900 μm^2 areas of cortex and hippocampus. Experimenters were blinded to drugging and analysis. Six to eight sections per mouse were analyzed and for each section 5 ROIs were analyzed in the cortex and 2 ROIs in the hippocampus using the cell counter tool in Image J [44]. This number of ROIs prevents the selection of only densely stained regions.

Immunoblotting

A brain hemisphere or neuronal culture dish was lysed in ice-cold lysis buffer (50 mM Tris, pH 8, 150 mM NaCl, and 1% Triton X-100) containing protease inhibitors cocktail (100 µM AEBSF, 2 µM leupeptin, 80 nM aprotinin, 5 µM Bestatin, 1.5 µM E-64 and 1 µM pepstatin A) and phosphatase inhibitors (10 mM NaF and 500 µM Na_3VO_4) and centrifuged twice for 10 min each at 20,000 xg and 4 °C. The supernatant was collected and total protein levels were quantified using Bradford Protein Assay. Homogenates were diluted in a mix of lysis buffer and β-mercaptoethanol containing 3x loading buffer and boiled for 10 min at 95 °C. Aliquots containing 30-40 µg total proteins were resolved by electrophoresis on a 7.5% or 10% SDS-polyacrylamide gel (SDS-PAGE) and transferred onto nitrocellulose membranes. Blots were blocked in Tris-

buffered saline, pH 7.6 containing 0.05% of Tween 20 (TBST) and 5% non-fat dry milk for 2 h at room temperature and then incubated overnight at 4 °C with primary antibodies diluted 1:1000 in TBST containing 2% non-fat dry milk. Immunodetection was performed by incubating with secondary antibodies (anti-rabbit/mouse) diluted 1:5000 in TBST containing 1% of non-fat dry milk for 1 h. Membranes were washed in TBST and then bands were detected and quantified using SuperSignal™ West Pico PLUS Chemiluminescent Substrate using Bio-Rad chemiluminescence system.

Embryo sex determination for primary culture

DNA was extracted from embryonic tissue by incubation overnight at 55 ºC in DNA lysis buffer (50 mM Tris-HCl, pH 8, 10 mM EDTA, 20 mM NaCl and 0.031% SDS) supplemented with Proteinase K. After incubation, lysates were centrifuged at 20,000 xg for 10 min at 25 °C and the supernatant was collected. DNA was precipitated by Isopropanol and was collected by centrifugation at 10,000 xg for 10 min at 4 °C. Tris-EDTA buffer (10 mM Tris-HCl, pH 8 and 1 mM EDTA, pH 8) was added to DNA, heated at 55 ºC for 10 min and then used for the PCR reaction. Primers were designed flanking an 84 bp deletion of the X-linked *Rbm31x* gene relative to its Y-linked gametolog *Rbm31y* (Forward; CACCTTAAGAACAAGCCAATACA and Reverse: GGCTTGTCCTGAAAACATTTGG) [30]. Following the PCR reaction, products were separated on an agarose gel containing RedSafe DNA stain (FroggaBio) and visualized on Bio-Rad fluorescence system.

Primary neuronal culture experiment

Following 12-15 days incubation, cultures were starved in HBSS for 1h. Cells were then treated with 10 µM CTEP or DMSO (vehicle for CTEP) for 30 min followed by 100 nM Aβ for 1 h at 37 °C. Human Aβ oligomers were prepared as per the manufacturer's recommendations.

Following this treatment, neuronal cultures were lysed with ice-cold RIPA buffer supplemented with protease and phosphatase inhibitors then immunoblotting was performed.

Radioligand binding

Radioligand binding was performed as previously described [45]. Briefly, cells washed with PBS and ice-cold lysis buffer (10 mM Tris–HCl, pH 7.4 and 5 mM EDTA, pH 8.0) was used to detach the cells. Cortex from mice and human were homogenized in ice-cold lysis buffer. To prepare the crude membrane preparation, cell or brain lysates were centrifuged twice at 40,000 xg for 20 min at 4 °C and supernatant was discarded after each centrifugation and the pellets were resuspended in lysis buffer. The crude membrane preparations were then suspended in resuspension buffer (62.5 mM Tris–HCl, pH 7.4 and 1.25 mM EDTA, pH 8.0) and kept on ice. The binding reactions were performed in duplicate by incubating crude membranes with 3 nM [^{3}H]-MPEP and increasing concentrations of either MPEP or Aβ oligomers in binding buffer (62.5 mM Tris–HCl, pH 7.4 and 1.25 mM EDTA, pH 8.0, 200 mM NaCl, 6.7 mM $MgCl_2$, 2.5 mM $CaCl_2$ and 8.33 mM KCl) at room temperature for 90 min. The nonspecific binding was determined using 10 µM MPEP. The binding reactions were terminated by rapid filtration through Whatman GF/C glass fiber filter sheets using semi-automated harvesting system (Brandel). The tritium-bound radioactivity was then counted using liquid scintillation counter (Beckman). The data were analyzed using GraphPad Prism and the equilibrium dissociation constant (Ki, M) of MPEP and Aβ were determined.

Co-immunoprecipitation

Hippocampus from male and female WT and mGluR5$^{-/-}$ mice were dissected and lysed in non-denaturing lysis buffer containing protease inhibitors provided with co-immunoprecipitation kit. Lysates were rotated for 1 hour at 4 °C and centrifuged at 10,000 g for 10 min at 4 ºC to pellet insoluble material. Precleared supernatant (500µg) was incubated with 1 µg of anti-PrP^c antibody

over night at 4 °C. Freshly washed protein A/G-sepharose beads were added to lysate/antibody mixture and samples were rotated for 2 hours at 4 °C. Beads were washed with wash buffer provided in the kit and then boiled with 3x loading buffer containing β-mercaptoethanol for 10 min at 90 °C. Samples were separated by SDS-PAGE and immunoblotted to identify co-immunoprecipitated mGluR5. An additional immunoblot was performed to examine mGluR5 and PrP^c protein expression in lysates prepared before incubation with antibody.

Statistical analysis

Means ± SEM are shown for each of independent experiments are shown in the various figure legends. GraphPad Prism 8 was used to analyze data for normality and statistical significance. Data normality was tested using Anderson-Darling and D'Agostino-Pearson omnibus tests and statistical significance was determined by two-way ANOVA, Student's t test or Kruskal-Wallis test as appropriate for the significant main interactions. Statistical details of individual experiments can be found in figure legends

REFERENCES

1. Rizzi, L., Rosset, I. & Roriz-Cruz, M. Global Epidemiology of Dementia: Alzheimer's and Vascular Types. *Biomed Res. Int.* **2014**, 1–8 (2014).

2. Casey, D. A., Antimisiaris, D. & O'Brien, J. Drugs for Alzheimer's disease: are they effective? *P T* **35**, 208–11 (2010).

3. Lanctôt, K. L., Rajaram, R. D. & Herrmann, N. Therapy for Alzheimer's Disease: How Effective are Current Treatments? *Ther. Adv. Neurol. Disord.* **2**, 163–80 (2009).

4. Hunter, S. & Brayne, C. Understanding the roles of mutations in the amyloid precursor protein in Alzheimer disease. *Mol. Psychiatry* (2017). doi:10.1038/mp.2017.218

5. Hamilton, A., Zamponi, G. W. & Ferguson, S. S. G. Glutamate receptors function as scaffolds for the regulation of β-amyloid and cellular prion protein signaling complexes. *Mol. Brain* **8**, 18 (2015).

6. Polanco, J. C. *et al.* Amyloid-β and tau complexity — towards improved biomarkers and targeted therapies. *Nat. Rev. Neurol.* **14**, 22–39 (2017).

7. Podcasy, J. L. & Epperson, C. N. Considering sex and gender in Alzheimer disease and other dementias. *Dialogues Clin. Neurosci.* **18**, 437–446 (2016).

8. Fisher, D. W., Bennett, D. A. & Dong, H. Sexual dimorphism in predisposition to Alzheimer's disease. *Neurobiol. Aging* **70**, 308–324 (2018).

9. Vest, R. S. & Pike, C. J. Gender, sex steroid hormones, and Alzheimer's disease. *Horm. Behav.* **63**, 301–307 (2013).

10. Hampel, H. *et al.* Precision medicine and drug development in Alzheimer's disease: the importance of sexual dimorphism and patient stratification. *Front. Neuroendocrinol.* **50**,

31–51 (2018).

11. Laws, K. R., Irvine, K. & Gale, T. M. Sex differences in cognitive impairment in Alzheimer's disease. *World J. Psychiatry* **6**, 54 (2016).

12. Tang, Y. *et al.* Estrogen-related receptor alpha is involved in Alzheimer's disease-like pathology. *Exp. Neurol.* **305**, 89–96 (2018).

13. Kelly, J. F. *et al.* Levels of estrogen receptors alpha and beta in frontal cortex of patients with Alzheimer's disease: relationship to Mini-Mental State Examination scores. *Curr. Alzheimer Res.* **5**, 45–51 (2008).

14. Rapp, S. R. *et al.* Effect of estrogen plus progestin on global cognitive function in postmenopausal women: the Women's Health Initiative Memory Study: a randomized controlled trial. *JAMA* **289**, 2663–72 (2003).

15. McCarrey, A. C. & Resnick, S. M. Postmenopausal hormone therapy and cognition. *Horm. Behav.* **74**, 167–172 (2015).

16. Podcasy, J. L. & Epperson, C. N. Considering sex and gender in Alzheimer disease and other dementias. *Dialogues Clin. Neurosci.* **18**, 437–446 (2016).

17. Niswender, C. M. & Conn, P. J. Metabotropic Glutamate Receptors: Physiology, Pharmacology, and Disease. *Annu. Rev. Pharmacol. Toxicol.* **50**, 295–322 (2010).

18. Um, J. W. *et al.* Metabotropic Glutamate Receptor 5 Is a Coreceptor for Alzheimer Aβ Oligomer Bound to Cellular Prion Protein. *Neuron* **79**, 887–902 (2013).

19. Haas, L. T., Kostylev, M. A. & Strittmatter, S. M. Therapeutic molecules and endogenous ligands regulate the interaction between brain cellular prion protein (PrPC) and metabotropic glutamate receptor 5 (mGluR5). *J. Biol. Chem.* **289**, 28460–28477 (2014).

20. Renner, M. *et al.* Deleterious effects of amyloid beta oligomers acting as an extracellular scaffold for mGluR5. *Neuron* **66**, 739–54 (2010).

21. Abd-Elrahman, K. S., Hamilton, A., Vasefi, M. & Ferguson, S. S. G. Autophagy is increased following either pharmacological or genetic silencing of mGluR5 signaling in Alzheimer's disease mouse models. *Mol. Brain* **11**, (2018).

22. Hamilton, A., Esseltine, J. L., DeVries, R. A., Cregan, S. P. & Ferguson, S. S. G. Metabotropic glutamate receptor 5 knockout reduces cognitive impairment and pathogenesis in a mouse model of Alzheimer's disease. *Mol. Brain* **7**, 40 (2014).

23. Hamilton, A. *et al.* Chronic Pharmacological mGluR5 Inhibition Prevents Cognitive Impairment and Reduces Pathogenesis in an Alzheimer Disease Mouse Model. *Cell Rep.* **15**, 1–7 (2016).

24. Zhang, Y. *et al.* Rapamycin upregulates glutamate transporter and IL-6 expression in astrocytes in a mouse model of Parkinson's disease. *Cell Death Dis.* **8**, e2611–e2611 (2017).

25. Abd-Elrahman, K. S., Hamilton, A., Albaker, A. & Ferguson, S. S. G. mGluR5 Contribution to Neuropathology in Alzheimer Mice Is Disease Stage-Dependent. *ACS Pharmacol. Transl. Sci.* (2020). doi:10.1021/acsptsci.0c00013

26. Lindemann, L. *et al.* CTEP: a novel, potent, long-acting, and orally bioavailable metabotropic glutamate receptor 5 inhibitor. *J. Pharmacol. Exp. Ther.* **339**, 474–86 (2011).

27. Jankowsky, J. L. *et al.* Mutant presenilins specifically elevate the levels of the 42 residue beta-amyloid peptide in vivo: evidence for augmentation of a 42-specific gamma secretase. *Hum. Mol. Genet.* **13**, 159–70 (2004).

28. Abd-Elrahman, K. S. *et al.* mGluR5 antagonism increases autophagy and prevents disease progression in the *zQ175* mouse model of Huntington's disease. *Sci. Signal.* **10**, eaan6387 (2017).

29. Zhang, T. *et al.* G-protein-coupled receptors regulate autophagy by ZBTB16-mediated ubiquitination and proteasomal degradation of Atg14L. *Elife* **4**, e06734 (2015).

30. Tunster, S. J. Genetic sex determination of mice by simplex PCR. *Biol. Sex Differ.* **8**, 31 (2017).

31. Insel, P. A., Tang, C.-M., Hahntow, I. & Michel, M. C. Impact of GPCRs in clinical medicine: Monogenic diseases, genetic variants and drug targets. *Biochim. Biophys. Acta - Biomembr.* **1768**, 994–1005 (2007).

32. Haas, L. T. *et al.* Silent Allosteric Modulation of mGluR5 Maintains Glutamate Signaling while Rescuing Alzheimer's Mouse Phenotypes. *Cell Rep.* **20**, 76–88 (2017).

33. Quiroz, J. A. *et al.* Efficacy and Safety of Basimglurant as Adjunctive Therapy for Major Depression. *JAMA Psychiatry* **73**, 675 (2016).

34. Youssef, E. A. *et al.* Effect of the mGluR5-NAM Basimglurant on Behavior in Adolescents and Adults with Fragile X Syndrome in a Randomized, Double-Blind, Placebo-Controlled Trial: FragXis Phase 2 Results. *Neuropsychopharmacology* **43**, 503–512 (2018).

35. O'Brien, R. J. & Wong, P. C. Amyloid precursor protein processing and Alzheimer's disease. *Annu. Rev. Neurosci.* **34**, 185–204 (2011).

36. Nah, J., Yuan, J. & Jung, Y.-K. Autophagy in neurodegenerative diseases: from mechanism to therapeutic approach. *Mol. Cells* **38**, 381–9 (2015).

37. Nixon, R. A. The role of autophagy in neurodegenerative disease. *Nat. Med.* **19**, 983–997

(2013).

38. Li, Q., Liu, Y. & Sun, M. Autophagy and Alzheimer's Disease. *Cell. Mol. Neurobiol.* **37**, 377–388 (2017).

39. Orr, M. E. & Oddo, S. Autophagic/lysosomal dysfunction in Alzheimer's disease. *Alzheimers. Res. Ther.* **5**, 53 (2013).

40. Rubinsztein, D. C. *et al.* Autophagy and its possible roles in nervous system diseases, damage and repair. *Autophagy* **1**, 11–22 (2005).

41. Raka, F. *et al.* Ca2+/Calmodulin-dependent protein Kinase II interacts with group i Metabotropic Glutamate and facilitates Receptor Endocytosis and ERK1/2 signaling: Role of β-Amyloid. *Mol. Brain* **8**, 21 (2015).

42. Dunn, H. A., Orlandi, C. & Martemyanov, K. A. Beyond the ligand: Extracellular and transcellular G protein-coupled receptor complexes in physiology and pharmacology. *Pharmacol. Rev.* **71**, 503–519 (2019).

43. Chen, G. F. *et al.* Amyloid beta: Structure, biology and structure-based therapeutic development. *Acta Pharmacologica Sinica* **38**, 1205–1235 (2017).

44. Schneider, C. A., Rasband, W. S. & Eliceiri, K. W. NIH Image to ImageJ: 25 years of image analysis. *Nature Methods* **9**, 671–675 (2012).

45. Plouffe, B. & Tiberi, M. Functional analysis of human D1 and D5 dopaminergic G protein-coupled receptors: Lessons from mutagenesis of a conserved serine residue in the cytosolic end of transmembrane region 6. *Methods Mol. Biol.* **964**, 141–180 (2013).

Figure 1

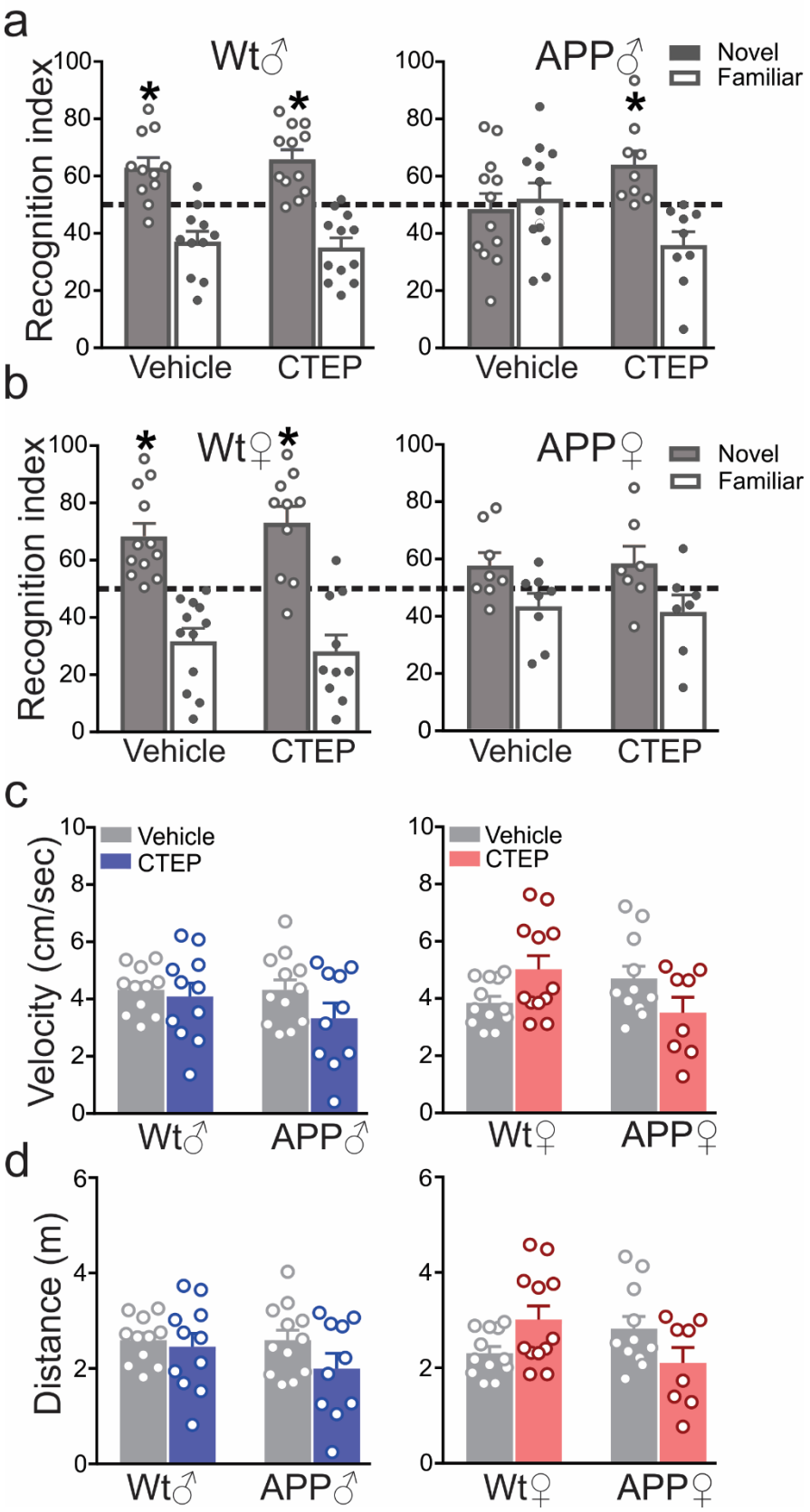
a
Wt♂
APP♂
Novel
Familiar
Recognition index
100
80
60
40
20
0
Vehicle
CTEP
b
Wt♀
APP♀
Novel
Familiar
Recognition index
Vehicle
CTEP
c
Vehicle
CTEP
Velocity (cm/sec)
10
8
6
4
2
0
Wt♂
APP♂
Wt♀
APP♀
d
Distance (m)
6
4
2
0
Wt♂
APP♂
Wt♀
APP♀

Figure 2

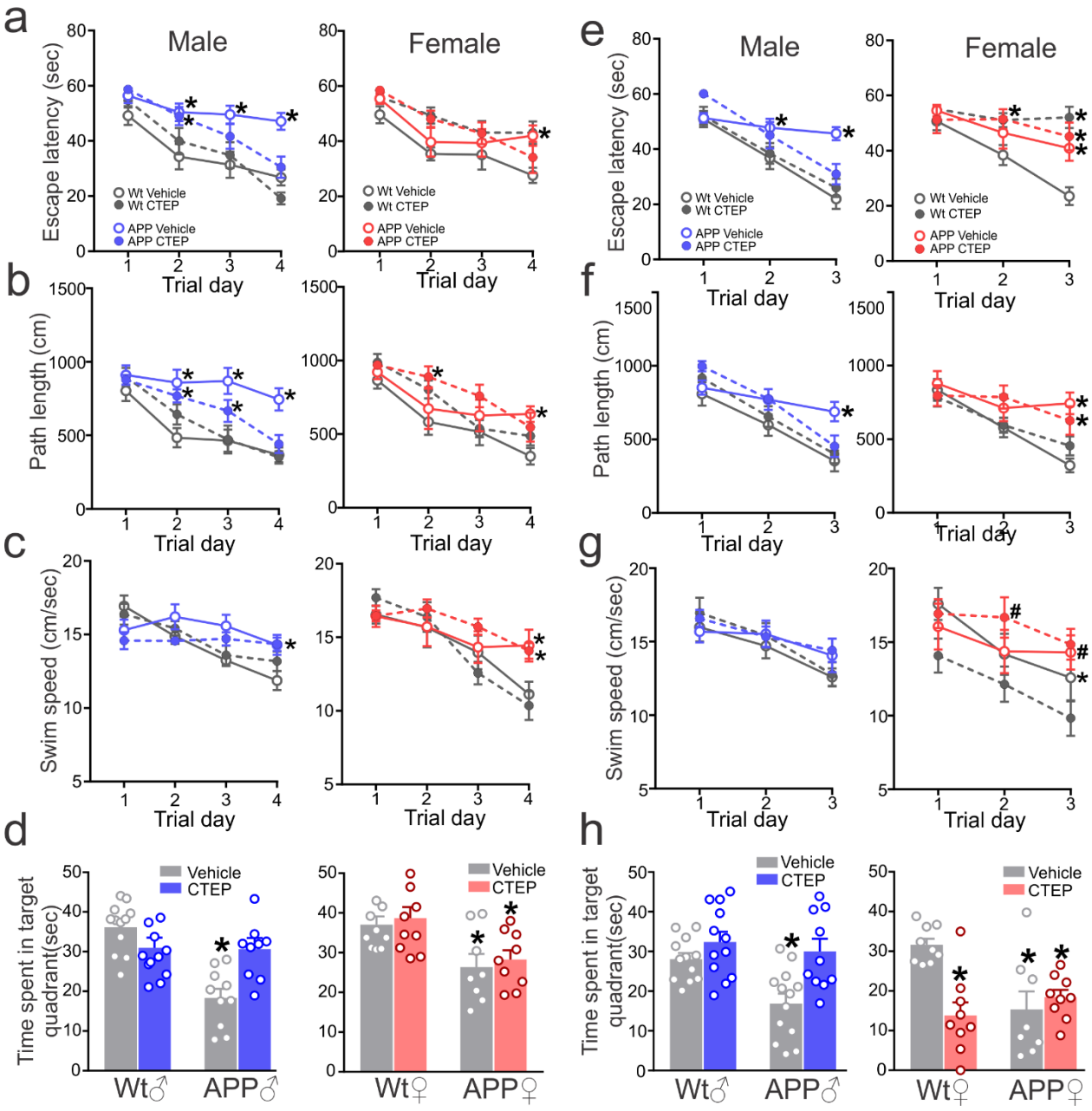
a
Male
Female
Escape latency (sec)
Wt Vehicle
Wt CTEP
APP Vehicle
APP CTEP
Trial day
b
Path length (cm)
c
Swim speed (cm/sec)
d
Time spent in target quadrant(sec)
Vehicle
CTEP
Wt♂
APP♂
Wt♀
APP♀
e
f
g
h

Figure 3

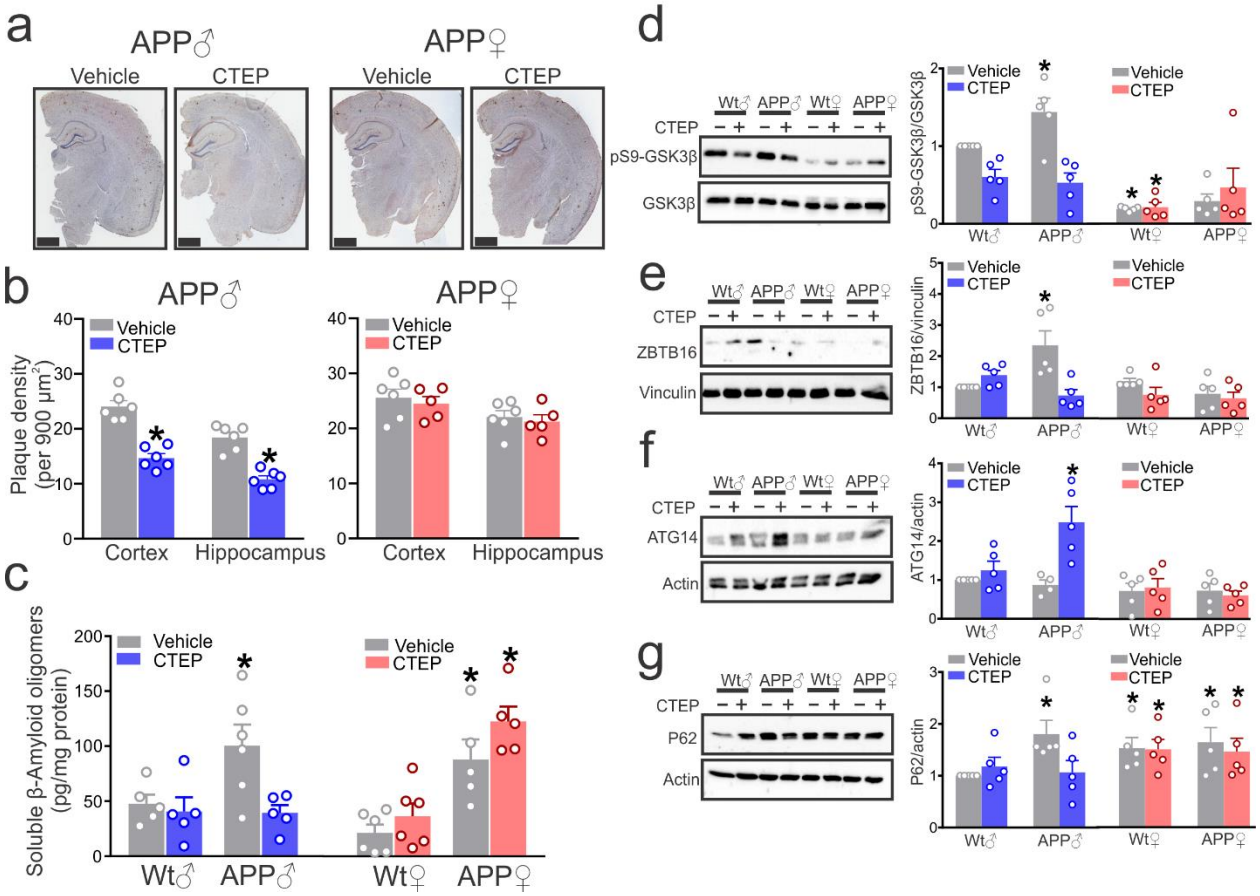
a
APP♂
APP♀
Vehicle
CTEP
b
Plaque density (per 900 μm²)
Cortex
Hippocampus
c
Soluble β-Amyloid oligomers (pg/mg protein)
Wt♂
APP♂
Wt♀
APP♀
d
CTEP
pS9-GSK3β
GSK3β
pS9-GSK3β/GSK3β
e
ZBTB16
Vinculin
ZBTB16/vinculin
f
ATG14
Actin
ATG14/actin
g
P62
P62/actin

Figure 4

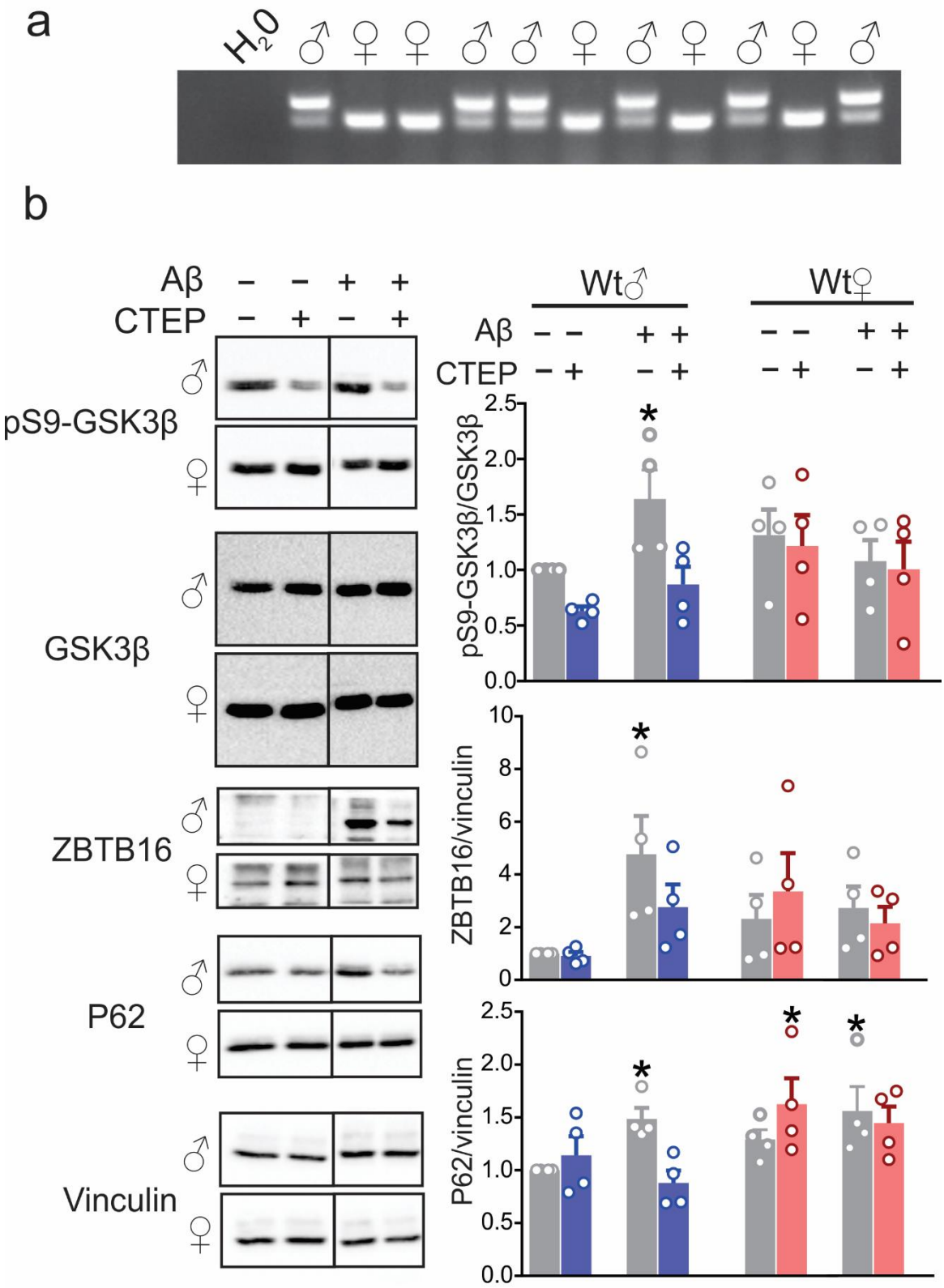
a
H2O
♂ ♀ ♀ ♂ ♂ ♀ ♂ ♀ ♂ ♀ ♂
b
Aβ − − + +
CTEP − + − +
pS9-GSK3β
GSK3β
ZBTB16
P62
Vinculin
Wt♂
Wt♀
pS9-GSK3β/GSK3β
ZBTB16/vinculin
P62/vinculin

Figure 5

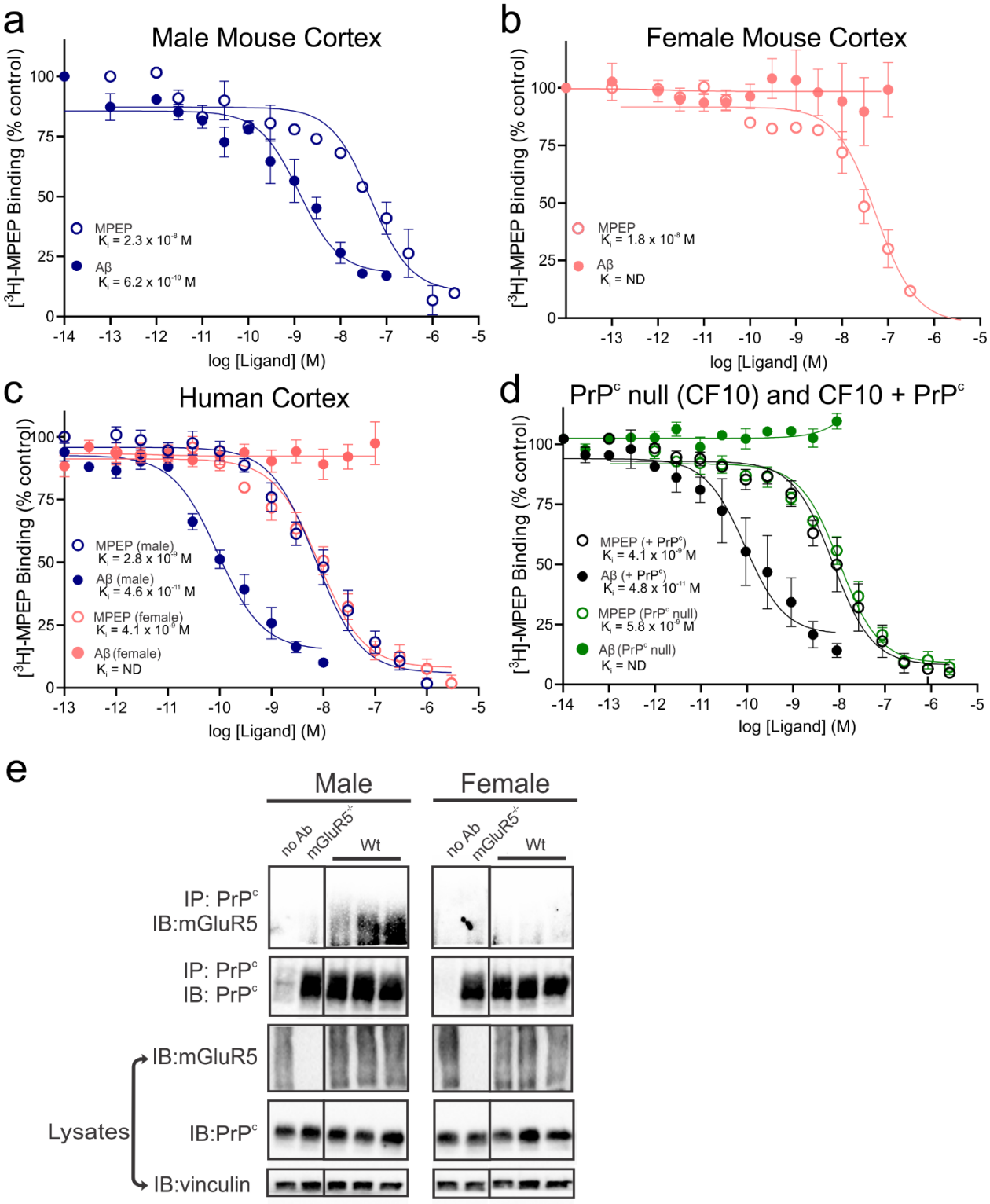
a
Male Mouse Cortex
[3H]-MPEP Binding (% control)
log [Ligand] (M)
MPEP
Ki = 2.3 x 10-8 M
Aβ
Ki = 6.2 x 10-10 M
b
Female Mouse Cortex
MPEP
Ki = 1.8 x 10-8 M
Aβ
Ki = ND
c
Human Cortex
MPEP (male)
Ki = 2.8 x 10-9 M
Aβ (male)
Ki = 4.6 x 10-11 M
MPEP (female)
Ki = 4.1 x 10-9 M
Aβ (female)
Ki = ND
d
PrPc null (CF10) and CF10 + PrPc
MPEP (+ PrPc)
Ki = 4.1 x 10-9 M
Aβ (+ PrPc)
Ki = 4.8 x 10-11 M
MPEP (PrPc null)
Ki = 5.8 x 10-9 M
Aβ (PrPc null)
Ki = ND
e
Male
Female
no Ab
mGluR5-/-
Wt
IP: PrPc
IB:mGluR5
IP: PrPc
IB: PrPc
IB:mGluR5
Lysates
IB:PrPc
IB:vinculin

Figure 6

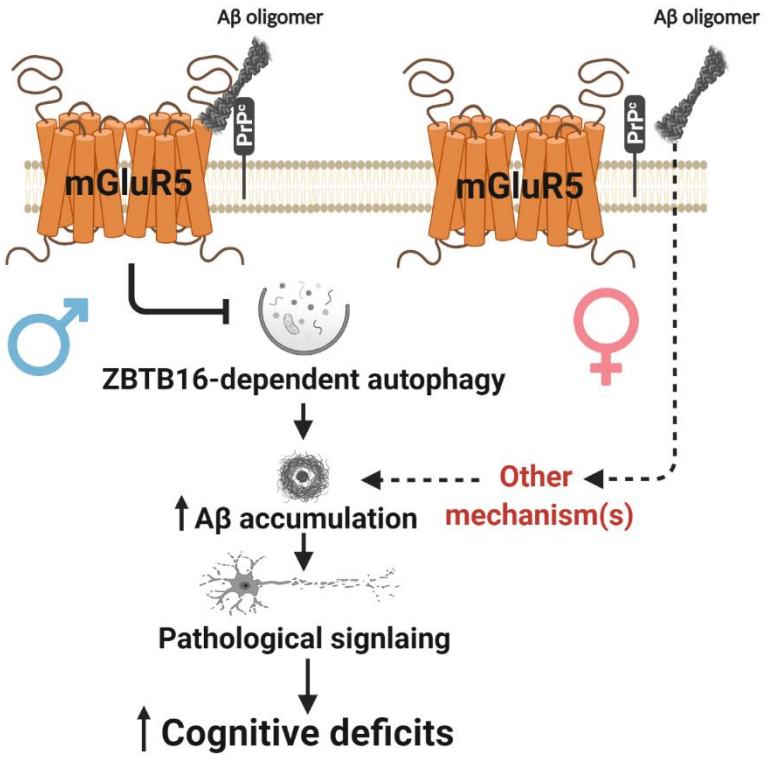
Aβ oligomer
Aβ oligomer
PrPc
PrPc
mGluR5
mGluR5
ZBTB16-dependent autophagy
Other
mechanism(s)
Aβ accumulation
Pathological signlaing
Cognitive deficits